Pathogens and Disease, 79, 2021, ftab058

https://doi.org/10.1093/femspd/ftab058
Advance Access Publication Date: 21 December 2021
Research Article

RESEARCH ARTICLE

Toxoplasma-proximal and distal control by GBPs in human macrophages

Daniel Fisch[1,2,†], Barbara Clough[1,2,!], Rabia Khan[2,#], Lyn Healy[3,$] and Eva-Maria Frickel[1,2,*,‡]

[1]Institute of Microbiology and Infection, School of Biosciences, University of Birmingham, Edgbaston B15 2TT, UK, [2]Host-Toxoplasma Interaction Laboratory, The Francis Crick Institute, London NW1 1AT, UK and [3]HESCU (Human Embryo and Stem Cell Unit), The Francis Crick Institute, London NW1 1AT, UK

[*]**Corresponding author:** Institute of Microbiology & Infection, School of Biosciences, The University of Birmingham, Edgbaston, Birmingham B15 2TT, UK. E-mail: e.frickel@bham.ac.uk

One sentence summary: In human macrophages, guanylate binging protein 1, 2 and 5 (GBP1/2/5) control the growth of the parasite *Toxoplasma gondii*, with solely GBP1 targeting the parasite vacuole for elimination.

Editor: Joern Coers

[†]Daniel Fisch, https://orcid.org/0000-0002-8155-0367
[!]Barbara Clough, https://orcid.org/0000-0002-3235-6170
[#]Rabia Khan, https://orcid.org/0000-0001-9230-6362
[$]Lyn Healy, https://orcid.org/0000-0002-7044-8789
[‡]Eva-Maria Frickel, https://orcid.org/0000-0002-9515-3442

ABSTRACT

Human guanylate binding proteins (GBPs) are key players of interferon–gamma (IFNγ)-induced cell intrinsic defense mechanisms targeting intracellular pathogens. In this study, we combine the well-established *Toxoplasma gondii* infection model with three *in vitro* macrophage culture systems to delineate the contribution of individual GBP family members to control this apicomplexan parasite. Use of high-throughput imaging assays and genome engineering allowed us to define a role for GBP1, 2 and 5 in parasite infection control. While GBP1 performs a pathogen-proximal, parasiticidal and growth-restricting function through accumulation at the parasitophorous vacuole of intracellular *Toxoplasma*, GBP2 and GBP5 perform a pathogen-distal, growth-restricting role. We further find that mutants of the GTPase or isoprenylation site of GBP1/2/5 affect their normal function in *Toxoplasma* control by leading to mis-localization of the proteins.

Keywords: guanylate binding protein; *Toxoplasma gondii*; GBP1; interferon; macrophage

INTRODUCTION

Human cells can defend themselves against pathogens in a process known as cell-intrinsic immunity (MacMicking 2012). Many proteins participating in this are induced by cytokine signaling such as signaling mediated by exposure to type II interferon–gamma (IFNγ; Ivashkiv 2018). Amongst IFNγ-induced proteins are several classes of immune GTPases, including the 63 kDa guanylate binding proteins (GBPs). Humans possess seven *GBP* genes (*GBP1-7*) located in a cluster on chromosome 1 (Olszewski, Gray and Vestal 2006). All GBPs have a similar structure with an N-terminal globular GTPase domain and an elongated C-terminal helical domain (Prakash *et al.* 2000). The GTPase hydrolyzes GTP to GDP which induces conformational changes of the proteins (Ghosh *et al.* 2006; Barz, Loschwitz and Strodel 2019; Ince *et al.* 2020). Furthermore, some GBP family members can also hydrolyze GDP to GMP, a unique feature of these

Received: 26 August 2021; **Accepted:** 17 December 2021

proteins (Schwemmle and Staeheli 1994; Praefcke *et al.* 2004; Abdullah, Balakumari and Sau 2010; Wehner and Herrmann 2010). The human GBPs 1, 2 and 5 have a CaaX-box at their C-terminus, which can be modified with an isoprenyl anchor. This lipid tail, together with other sites of the proteins, e.g. a C-terminal polybasic motif R584–586 (Kohler *et al.* 2020), allows for membrane interaction. Moreover, GBPs are known to form dimers and homo-/hetero-oligomers as well as larger protein aggregates (Britzen-Laurent *et al.* 2010; Kravets *et al.* 2016; Ince *et al.* 2017; Wandel *et al.* 2017; Kutsch *et al.* 2020). Some family members are known to target cytosolic and vacuolar bacterial, viral or protozoal pathogens within cells which leads to their disruption and exposure (Tretina *et al.* 2019). Other functions of GBPs include modulation of apoptosis and pyroptosis, cytokine production, autophagy, radical production and energy metabolism (Tretina *et al.* 2019). Altogether, they contribute to efficient control of intracellular pathogens.

One common intracellular pathogen of humans is the apicomplexan parasite *Toxoplasma gondii* (Tg), with roughly 30% of humans suffering from non-symptomatic, persistent infection (Pappas, Roussos and Falagas 2009). Tg has an atypical population structure with three major clonal lineages that differ in virulence: type I, II and III are the predominant lines in Europe and North America (Sibley and Boothroyd 1992; Howe and Sibley 1995; Sibley and Ajioka 2008). Type II strains are the most common in human infection. Infection with type I strains are rare, although they display the highest virulence in mice (Sibley and Boothroyd 1992; Howe and Sibley 1995). Tg has a more genetically diverse population structure in South America (Lehmann *et al.* 2006; Pena *et al.* 2008). Globally, Tg appears in six major clades with 16 haplotypes that display distinct geographic distribution patterns (Su *et al.* 2012).

Tg grows intracellularly once it has infected a human host, forming its own subcellular compartment known as the parasitophorous vacuole (PV; Sibley 2011). Within the PV, Tg is protected from detection by cytosolic pattern recognition receptors and the innate immune system (Clough and Frickel 2017). While asymptomatic in immune-competent hosts, where Tg transforms into a dormant infection forming tissue cysts in brain and muscle, the parasite can cause the disease known as toxoplasmosis in immunocompromised individuals. Moreover, recurring ocular infections with Tg are a common morbidity in South America, as are complications upon new infection with Tg during pregnancy (Desmonts *et al.* 1985; Daffos *et al.* 1988; Remington *et al.* 2011). Tg infection control in humans critically depends on a cell-mediated immune response and on the cytokine IFNγ (Gazzinelli *et al.* 1993, 1994; Hunter *et al.* 1994; Wilson, Matthews and Yap 2008). Tg is therefore a good model pathogen to assess the function of human GBPs.

Macrophages are key cells of the innate immune system. They derive from monocytes infiltrating an inflamed/infected tissue and serve several purposes: macrophages (1) phagocytose pathogens and reduce the infectious burden (Rosales and Uribe-Querol 2017), (2) produce cytokines that prime the immune response (Wynn, Chawla and Pollard 2013), (3) present antigens for activation of the adaptive immune response (Roche and Furuta 2015; Hughes *et al.* 2016), (4) clear debris from dead cells (Green, Oguin and Martinez 2016) and (5) contribute to healing of damaged tissues (Feghali and Wright 1997; Cronkite and Strutt 2018). IFNγ which is produced in large amounts during a cell-mediated immune response (Dinarello 2007; Turner *et al.* 2014), activates and polarizes macrophages, and is the key inducer-cytokine for GBPs (Cheng *et al.* 1985; Darnell, Kerr and Stark 1994; Boehm *et al.* 1998). Therefore, GBP-expressing macrophages frequently encounter Tg and are a well-suited cell type to study GBP functions with sufficient physiological relevance.

Several model cell lines and systems are used to study macrophage biology. One of the most used is the monocytic cancer cell line THP-1 (Chanput, Mes and Wichers 2014). Since long-term culture induces unwanted genetic drift, culture of THP-1 is usually restricted to fewer passages (Ben-David *et al.* 2018; Noronha *et al.* 2020). THP-1 monocytes can be terminally differentiated using phorbol 12-myristate 13-acetate (PMA), a small molecule, irreversible activator of PKC (Ryves *et al.* 1991). Hence, PMA needs to be employed at the minimal concentration necessary for differentiation, in order to reduce activation of cells and so avoid masking any effects of further activations (Park *et al.* 2007). Use of THP-1 cells allows for genome-editing but has the disadvantage of using immortalized cells. Newer systems instead use induced pluripotent stem cells (iPSC). The KOLF iPS cell line can be maintained in culture indefinitely and can be transformed into embryonic bodies (EBs), which upon addition of a cytokine cocktail work as monocyte production factories. Monocytes can be harvested weekly or fortnightly, and then terminally differentiated into macrophages with M-CSF (Wilgenburg *et al.* 2013). This produces primary-like human cells. Lastly, primary cells can be used for macrophage biology research. To obtain these, leukocytes are enriched from healthy donor blood. From this, peripheral blood mononuclear cells (PBMCs) can be purified by density-gradient centrifugation from which monocytes are isolated based on surface expression of CD14. These can be terminally differentiated into monocyte-derived macrophages (MDMs). Since MDMs are primary cells, they most accurately reflect human biology. Combining these systems allows for an optimal *in vitro* study of human macrophage biology (Tedesco *et al.* 2018).

We have previously shown that GBP1 is recruited to the type I and II Tg PV in human macrophages, disrupts both the PV membrane and the plasma membrane of the parasite leading to parasite DNA detection by AIM2 and programmed cell death by apoptosis (Fisch *et al.* 2019a, 2020). It was not clear what impact GBPs have on parasite control in human macrophages. In this study, we combine the three distinct macrophage models with gene silencing, genome engineering and high-throughput imaging to delineate the contribution of human GBPs and their mutants to control of Tg infection. We demonstrate that isoprenylated GBPs control the in-part uncoupled processes of Tg growth restriction and parasite killing, critically depending on their correct subcellular localization. Using panels of GBP mutants, we show that GTPase activity and isoprenylation dictate GBP localization and their pathogen-proximal and -distal roles in cell-intrinsic immunity.

RESULTS

Human GBP1, 2 and 5 restrict *Toxoplasma* growth in human macrophages and human GBP1 reduces *Toxoplasma* parasite vacuole numbers

To study the function of human GBPs in the context of controlling Tg infection, we utilized three distinct human macrophage culture systems: PMA-differentiated THP-1 macrophages, KOLF iPSC and *in vitro* differentiated macrophages of purified primary CD14$^+$ monocytes from blood of healthy donors (Figure S1A, Supporting Information). Flow cytometry analysis confirmed presence of the surface markers CD14, FcγRIII (CD16) and CD68 in all macrophage models (Figure S1B, Supporting Information). RT-qPCR analysis of *GBP* expression after IFNγ-treatment of the

cells showed induction of expression for *GBP1–5*, but no expression of *GBP6* or *GBP7* in any of the three macrophage models (Figures S1C and D, Supporting Information; Fisch *et al.* 2019a). In all cells, *GBP1* and *GBP2* had the highest total expression levels, followed by *GBP5* (Figure S1C, Supporting Information). Interestingly, the non-isoprenylated *GBPs 3* and 4 had the lowest total expression levels in all macrophage models (Figure S1C, Supporting Information). Of all GBPs, *GBP5* showed the highest IFNγ-inducibility, which can be explained by the near complete absence of its transcript in naïve macrophages (Figure S1D, Supporting Information). *GBP3* consistently showed the lowest expression induction (Figure S1D, Supporting Information).

Having confirmed expression of *GBP1* through 5 following IFNγ-treatment of human macrophages, we next used our previously established RNA interference assay, to specifically deplete cells of individual GBPs (Fisch *et al.* 2019a) and assessed their influence on Tg-growth control using high-throughput imaging and analysis with HRMAn (Fisch *et al.* 2019b, 2021). *GBP* silencing efficiency was comparable to our previously published data in THP-1 cells (Fisch *et al.* 2019a) for all macrophage models (Figure S1E, Supporting Information). With this assay we could establish that silencing of *GBP1*, *GBP2* or *GBP5* expression led to a loss of parasite growth restriction (Fig. 1A) and replication restriction (Fig. 1B) in all cell lines tested. Since tissue culture cells can be infected multiple times (i.e. contain more than one vacuole), we use the ratio between vacuoles and cells to measure the capacity of the cells to kill intracellular Tg. Depletion of GBP1 additionally reduced this ability of all IFNγ-primed macrophages to kill intracellular parasites, while GBP2 and 5 contributed to this function to a lesser extent in THP-1 and iPSC macrophages only (Fig. 1C). Thus, we concluded that GBP1, 2 and 5-depletion significantly restricts Tg growth in the macrophage models, while GBP1 additionally kills Tg in all three macrophage models by reducing the vacuole/cell ratio.

To scrutinize the results obtained using our high-throughput imaging approach, we also determined Tg fitness with traditional plaque assays (Figure S1F, Supporting Information). We could confirm our observation that GBP1, GBP2 and GBP5 exert Tg-growth control in IFNγ-primed THP-1 macrophages (Figure S1F, Supporting Information).

Addition of IFNγ is necessary for restoring *Toxoplasma* growth restriction, but not parasite vacuole numbers when re-expressing GBPs in knockout cells

To further assess the influence of GBP1, 2 and 5 in controlling Tg infection in macrophages, we next assessed THP-1 CRISPR knockout cell lines of the respective gene. THP-1Δ*GBP1* and Δ*GBP5* were previously published (Fisch *et al.* 2019a; Krapp *et al.* 2016) and Δ*GBP2* cells were created using the LentiCRISPR-v2 system. All cell lines were characterized by immunoblotting (Figure S2A, Supporting Information), RT-qPCR (Figure S2B, Supporting Information), genotyping PCRs (Figure S2C, Supporting Information) and Sanger sequencing (Figures S2D and E, Supporting Information) to confirm absence of the protein and no off-target effects on the other GBP family members. Of note, the knockout cells were created with different approaches, where the *GBP1* gene has a major truncation, *GBP2* is entirely deleted and *GBP5* has nonsense mutations, all rendering the respective gene product absent (Figure S2, Supporting Information). Immunoblotting the cell lines side-by-side also confirmed presence of the non-targeted GBP proteins in the knockout cells (Figure S2F, Supporting Information) as had been observed using qPCR for the transcripts (Figure S2B, Supporting Information). Next, we used our previously described Doxycycline (Dox)-inducible system (Fisch *et al.* 2019a) and reconstituted the knockout cells with the respective GBP family member (Figure S2G, Supporting Information). Using these cells in our high-throughput imaging assay, we were able to replicate the previous observation of a loss of Tg-growth and replication restriction in the Δ*GBP1*, Δ*GBP2* and Δ*GBP5* cells which could be reversed by expression induction through addition of Dox (Fig. 2A and B). Interestingly, addition of Dox alone (expression of just the single GBP) was not sufficient and additional IFNγ-treatment was required (Fig. 2A and B). This might indicate that several GBPs act in concert or that another IFNγ-inducible factor is required. For parasite killing on the other hand, GBP1 expression alone through Dox-induction could fully reverse the loss of vacuole/cell control upon type II Tg infection (Fig. 2C). However, for type I Tg infection this was only fully restored to wildtype levels upon the extra addition of IFNγ (Fig. 2C). Complete ablation of GBP2 and 5 by CRISPR in THP-1 macrophages, in contrast to downregulation by siRNA, showed that these two GBPs are in fact not able to kill Tg *via* control of the vacuole/cell ratio (Figs 1D and 2C). Using HRMAn we further assessed the overall effect of GBP1, 2 and 5 on the total parasite load per cell (Fig. 2D). This measure combines replication–restriction and killing, and it was only reduced comparable to IFNγ-primed THP-1 WT, if Δ*GBP1*, Δ*GBP2* and Δ*GBP5* cells were treated with IFNγ+Dox. This again showed that for the overall control of the parasite burden GBP1 is essential for killing and growth restriction, whereas GBP2 and GBP5 were needed solely for growth restriction (Fig. 2D). In summary, human macrophages express GBPs 1–5 upon IFNγ-stimulation and GBP1, 2 and 5 all contribute to the growth control of the intracellular parasites, while GBP1 is additionally responsible for controlling vacuole numbers.

GTPase activity and lipidation of GBP1, 2 and 5 are essential for their anti-*Toxoplasma* activity

We next created panels of mutants for GBP1, GBP2 and GBP5 targeting their GTPase activity, C-terminal lipidation, the polybasic motif in GBP1 and its dimerization capacity (Fig. 3A). We transduced the respective Δ*GBPx* cells with the Dox-inducible system (Figure S3, Supporting Information). We then assessed the effect of these mutants on the functionality of the proteins (Fig. 3B–D). To do so, we performed our high-throughput imaging assay as before by treating THP-1 macrophages with IFNγ+Dox and normalized the resulting effects to the IFNγ-only treated control of the same cell line. In this way, the only difference is presence or absence of the wildtype or mutated GBP protein in otherwise IFNγ-primed cells. Like this, we were able to calculate the proportion of Tg-growth restriction, as measured by the vacuole size, or killing, as measured by determining the ratio between vacuoles and cells, of the respective GBP functionality relative to the absence of the same GBP (Fig. 3B–D).

Screening the GBP1 mutants showed that mutations rendering the GTPase activity non-functional (K51A, R48A, T75A, D184N or S52N) failed to restrict Tg growth and killing, whereas GTPase-mutants that predominantly affected GMP-production (E99A, D112A or D103L/D108L) still restricted the growth but failed to kill Tg. GBP1^{R48P} with a predicted inactive GTPase was still active to restrict and kill Tg, although slightly impaired in this capacity (Fig. 3B). Isoprenylation site mutations (C589A or Δ589–592) also failed to kill and restrict Tg-growth (Fig. 3B).

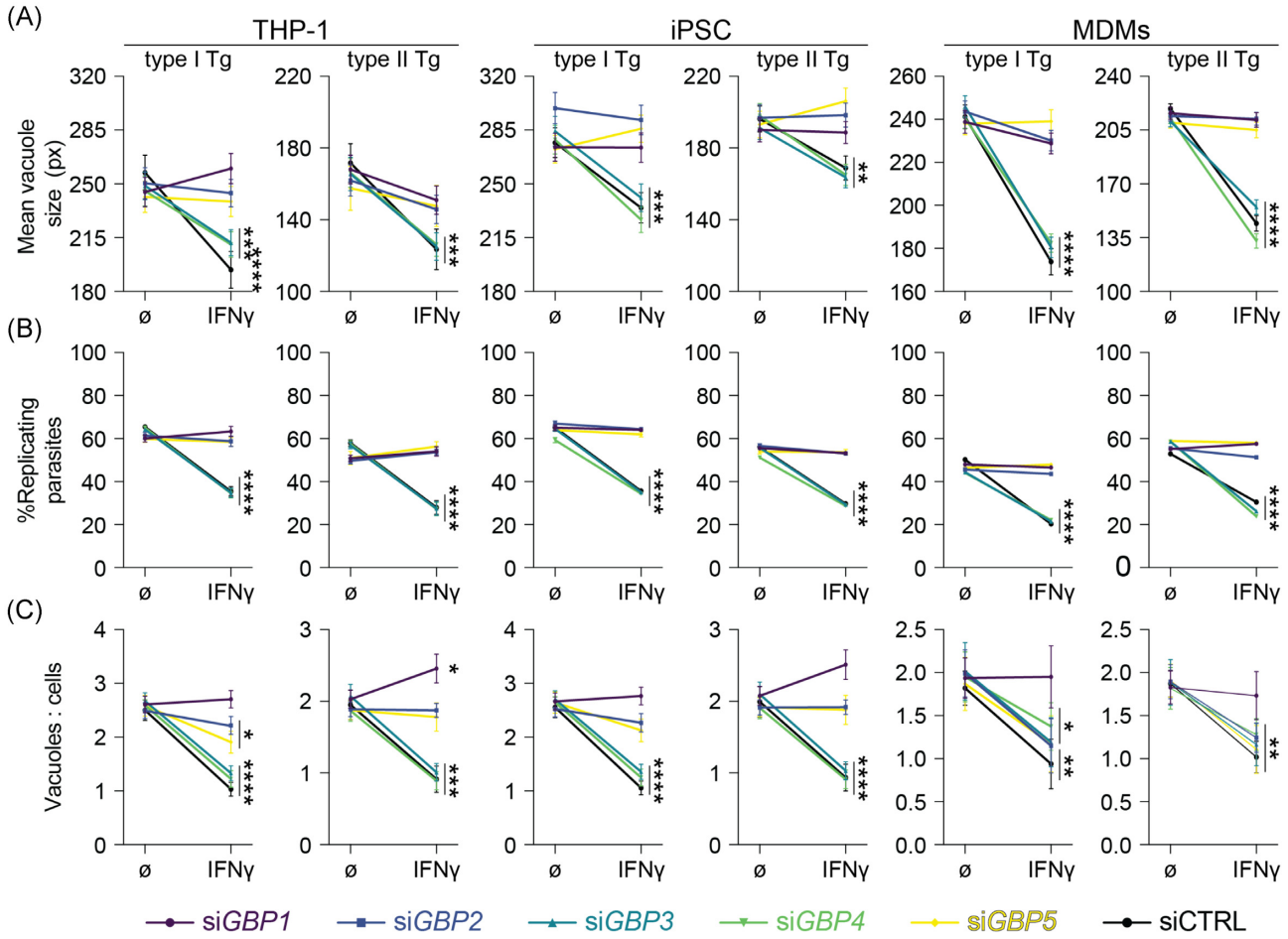

Figure 1. Selective human GBPs limit *Toxoplasma* parasite numbers and restrict their growth in human macrophages. HRMAn-based quantification of mean vacuole size **(A)**, proportion of replicating parasites **(B)** and ratio between vacuoles and cells **(C)** of THP-1, iPSC-derived or MDMs transfected with siRNA against the indicated *GBP* or non-targeting control (CTRL), untreated or primed with IFNγ and infected with type I (RH) or type II (PRU) *T. gondii* (Tg) at 18 h p.i. Data information: Graphs in (A–C) shown mean ± SEM from $n = 3$ independent experiments or $n = 4$ donors (MDMs). Owing to the high-throughput capability of HRMAn, at least 2000 individual host cells were analysed for each datapoint. *$P \leq 0.05$; **$P \leq 0.01$; ***$P \leq 0.001$ and ****$P \leq 0.0001$ in (A–C) from two-way ANOVA comparing unprimed to IFNγ-primed condition following adjustment for multiple comparisons.

GBP2 and GBP5 mutations that abolish GTP hydrolysis (K51A or D103L/D108L for GBP2 and KS51/52AA for GBP5) or mutations of the isoprenylation sites (C588A or Δ588–591 for both) failed to restrict Tg-growth (Fig. 3C and D). Since neither protein contributes to Tg-killing, this was unaffected and likely carried out by endogenous GBP1 induced through IFNγ-priming of the cells (Fig. 3C and D).

GBP2 and 5 do not localize to *Toxoplasma* vacuoles

Comparing findings of the GBP mutant screen indicates a close link between GBP1 GTPase activity/isoprenylation and the control of Tg reminiscent of previous results on GBP1 recruitment and correlation to Tg-killing and host cell death (Fisch *et al.* 2019a, 2020). This suggests a functional link between these processes. Thus, mCherry-tagged GBPx mutants, showing a pathogen growth control phenotype (affecting GTPase and isoprenylation), were created, and transduced into Δ*GBPx*+Tet cells to study the localization and spatiotemporal activities (Figure S4, Supporting Information). Using mCH-GBP1 WT, mCH-GBP2 WT and mCH-GBP5 WT expressing cells, we could confirm that GBP5 was localizing to the Golgi apparatus as had been described before in epithelial cells (Tripal *et al.* 2007; Britzen-Laurent *et al.* 2010; Fig. 4A). In IFNγ-primed, uninfected cells, GBP1 mutants of the GTPase or isoprenylation site appeared more dispersed in the cytosol instead of showing a granular appearance like GBP1 WT. This might indicate a loss of membrane interactions or aggregate formation (Fig. 4B). The observed dispersed cytoplasmic localization of GBP2 had no obvious differences with mutation of the protein, but GBP5 mutants affecting the GTPase or its isoprenylation had lost their localization at the Golgi (Fig. 4B).

In contrast to GBP1, neither GBP2 WT nor GBP5 WT recruited to Tg vacuoles in infected human macrophages implying that they have their growth restrictive function away from the pathogen (pathogen-distal; Fig. 4C). We, therefore, only assessed recruitment of GBP1 mutants to Tg. In agreement with our previous observations of correlation between modulation of macrophage cell death and GBP1 recruitment to pathogens (Fisch *et al.* 2019a, 2020), all GBP1 GTPase and isoprenylation mutants failed to target Tg vacuoles in IFNγ-primed THP-1 cells (Fig. 4D).

In summary, GBP1, 2 and 5 contributed to the control of Tg infection via parasite growth restriction and reduction of vacuole/cell numbers in three different human, *in vitro* macrophage models, including primary-like iPSCs and primary MDMs. Genome engineering and use of a Dox-inducible system

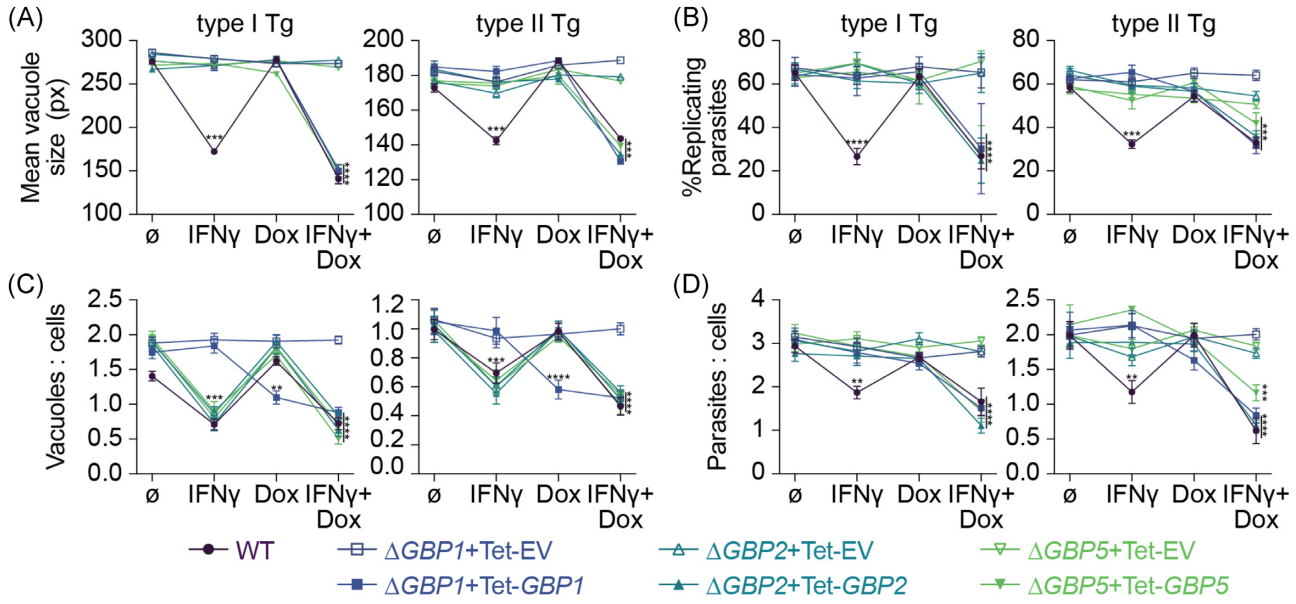

Figure 2. Re-expression of GBPs restores *Toxoplasma* restriction in Δ*GBP* cells. HRMAn-based quantification of mean vacuole size **(A)**, proportion of replicating parasites **(B)**, ratio between vacuoles and cells **(C)**, ratio between parasites and cells **(D)** of THP-1Δ*GBP1*, Δ*GBP2* or Δ*GBP5* cells transduced with Tet-empty vector (EV, open symbols) or Tet-*GBP1/2/5* (closed symbols) untreated or primed with IFNγ and/or Doxycycline (Dox) and infected with type I (RH) or type II (PRU) *T. gondii* (Tg) at 18 h p.i. Data information: graphs in (A–D) shown mean ± SEM from $n = 3$ independent experiments. $^{*}P \leq 0.05$; $^{**}P \leq 0.01$; $^{***}P \leq 0.001$ and $^{****}P \leq 0.0001$ for indicated condition in (A–D) from two-way ANOVA comparing to untreated condition following adjustment for multiple comparisons.

confirmed GBP1 targeting to pathogen vacuoles to depend on its GTPase activity and isoprenylation. Other infection- and IFNγ-treatment-dependent factors are likely involved in regulating its Tg control function. Furthermore, GBP1 needs to be able to produce GMP and be targeted to vacuoles to kill Tg parasites by reducing vacuole/cell numbers. Surprisingly, GBP2 and GBP5 did not target Tg vacuoles, but were involved in Tg growth restriction. This function depended on both GBP2 and GBP5 GTPase activity and isoprenylation.

DISCUSSION

Here, we employed three *in vitro* models to study the role of human GBPs in infected macrophages. Gene depletion experiments in THP-1 cells, MDMs and iPSC-derived macrophages established that GBP1, GBP2 and GBP5 control the replication of Tg, while GBP1 was additionally parasiticidal. The findings on pathogen control by GBPs were confirmed using THP-1 CRISPR KO cell lines and rescued by reconstituting protein expression. Use of an imaging-based assay also allowed to delineate the contribution of individual GBPs to restriction and/or killing, and extend observations made by overall pathogen burden assessment through classical plaque formation assays.

Following IFNγ-stimulation, macrophages express *GBP1–5*, but not *GBP6* or *GBP7*, which are predominantly expressed in the oropharyngeal tract (Uhlen *et al.* 2015) and which was expected since *GBP6/7* lack GAS elements in their promoter regions (Tretina *et al.* 2019). GBP expression patterns resembled expression profiles in mesenchymal stem cells (Qin *et al.* 2017). Our findings furthermore concur with previous studies showing an effect of human GBP1 on Tg growth in mesenchymal stem cells and in A549 lung epithelial cells (Johnston *et al.* 2016; Qin *et al.* 2017). A role for human GBP2 and GBP5 in Tg infection control has so far not been established, but a large body of literature suggests and supports a similar role for their murine homologues (Virreira Winter *et al.* 2011; Kravets *et al.* 2012, 2016; Degrandi *et al.* 2013; Matta *et al.* 2018).

The three GBP family members that can be isoprenylated (Nantais *et al.* 1996; Tripal *et al.* 2007; Britzen-Laurent *et al.* 2010) contributed to Tg growth restriction, while GBP3 and GBP4 did not. Moreover, these three GBPs were highly upregulated and expressed upon IFNγ-stimulation, while GBP3 and GBP4 show significantly lower expression and inducibility in all three human macrophage models studied here. This may indicate a different role for GBP3/4. One conceivable hypothesis is that GBP3/4 regulate lipidated GBPs through heterotypic interactions, partially resembling the Irg GTPase system of the mouse, in which GMS-Irgs control the activity of the GKS-Irgs (Hunn *et al.* 2008; Haldar *et al.* 2013, 2016).

It is likely that GBP1, 2 and 5 act in concert. siRNA-depletion and Dox-reconstitution experiments suggest that for growth restriction all three GBPs are needed, since depletion of a single member abolished restriction and conversely reconstitution of a single member did not rescue the loss of restriction in the CRISPR KO cells. Growth restriction alone was not able to reduce the overall parasite burden. For this to occur, Tg-killing mediated by GBP1 was required. Similar hierarchical organization of the human GBP system was observed during *Shigella flexneri* infection where the pathfinder GBP1 first targets the pathogen, thus facilitating recruitment of GBP2/3 and GBP4 (Piro *et al.* 2017; Wandel *et al.* 2017). It is likely that similar cooperation is needed between GBP1, 2 and 5 for the pathogen-distal action of GBP2 and 5 against Tg. Additionally, it is probable that GBP1 also has a pathogen-distal function for Tg growth restriction, as mutants that cannot produce GMP do not localize to the PV but still restrict the parasite growth. These GBP1 mutants therefore resemble the function of GBP2/5.

In uninfected cells GBP1, 2 and 5 showed differing localizations: GBP1 had a granular appearance suggesting aggregate formation or (endo-)membrane interaction, GBP2 was uniformly distributed in the cytosol and GBP5 associated with the Golgi

(A)

		Hydrolysis /WT	GTP ?	GDP ?	Effect	Source
GBP1	K51A	<0.05%	-	-	GTPase dead	Praefcke *et al*, 2004
	R48A	0.85%	-	-		
	E99A	6.63%	-	-		
	T75A	0.06%	-	-		
	D184N	23.15%	+	-	GTPase deficient	
	D112A	15.78%	+	-		
	S52N	0.10%	-	-	GTPase dead	
	R48P	0.50%	-	-		Modiano *et al*, 2005
	D103L/D108L	?	+	-	No GMP prod.	Abdullah *et al*, 2010
	Δ589-592	100%	+	+	No isoprenylation	Britzen-Laurent *et al*, 2010
	C589A	100%	+	+		
	RK227/228EE	100%	+	+	Dimeric	
	D192E	100%	+	+	No cleavage	Naschberger *et al*, 2017
	R584-586A	100%	+	+	polybasic motif	Piro *et al*, 2017
GBP2	K51A	<0.05%	-	-	GTPase dead	Britzen-Laurent *et al*, 2010
	Δ588-591	100%	+	+	No isoprenylation	
	C588A	100%	+	+		
	D103L/D108L	?	+	-	No GMP prod.	Abdullah *et al*, 2010
GBP5	KS51/52AA	<0.05%	-	-	GTPase dead	Wehner *et al*, 2010
	Δ588-591	100%	+	-	No isoprenylation	Britzen-Laurent *et al*, 2010
	C588A	100%	+	-		

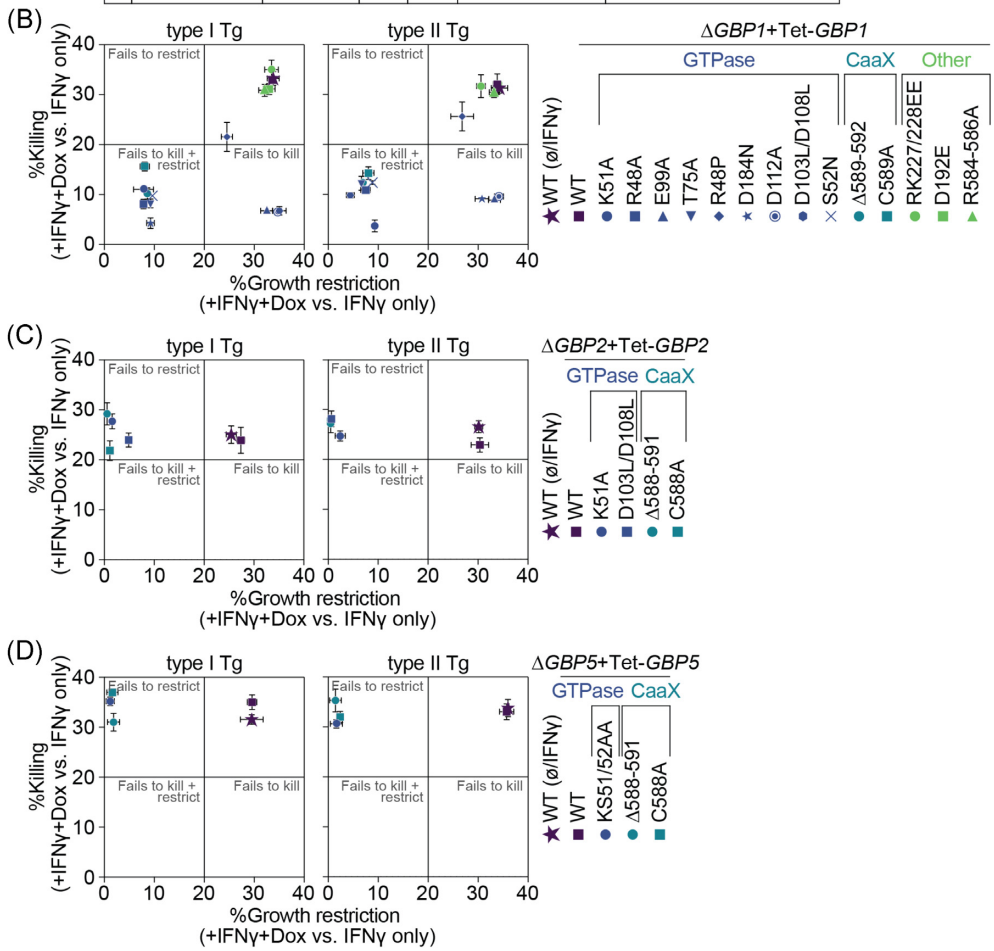

Figure 3. GTPase activity and lipidation of GBP1, 2 and 5 are essential for their anti-*Toxoplasma* activity. Overview of GBP1, GBP2 and GBP5 mutants **(A)**. Growth restriction and killing (= ratio between vacuoles and cells) of type I (RH) and type II (PRU) *T. gondii* (Tg) at 18 h p.i. in THP-1Δ*GBP1*+Tet-*GBP1* cells expressing the indicated mutant of GBP1 **(B)**, Δ*GBP2*+Tet-*GBP2* cells expressing the indicated mutant of GBP2 **(C)**, Δ*GBP5*+Tet-*GBP5* cells expressing the indicated mutant of GBP5 **(D)** or of IFNγ-treated THP-1 WT cells for each, plotted as proportion between IFNγ + Doxycycline (Dox)-treated versus IFNγ-only-treated cells. Data information: Graphs in (B–D) show mean ± SEM from $n = 3$ independent experiments.

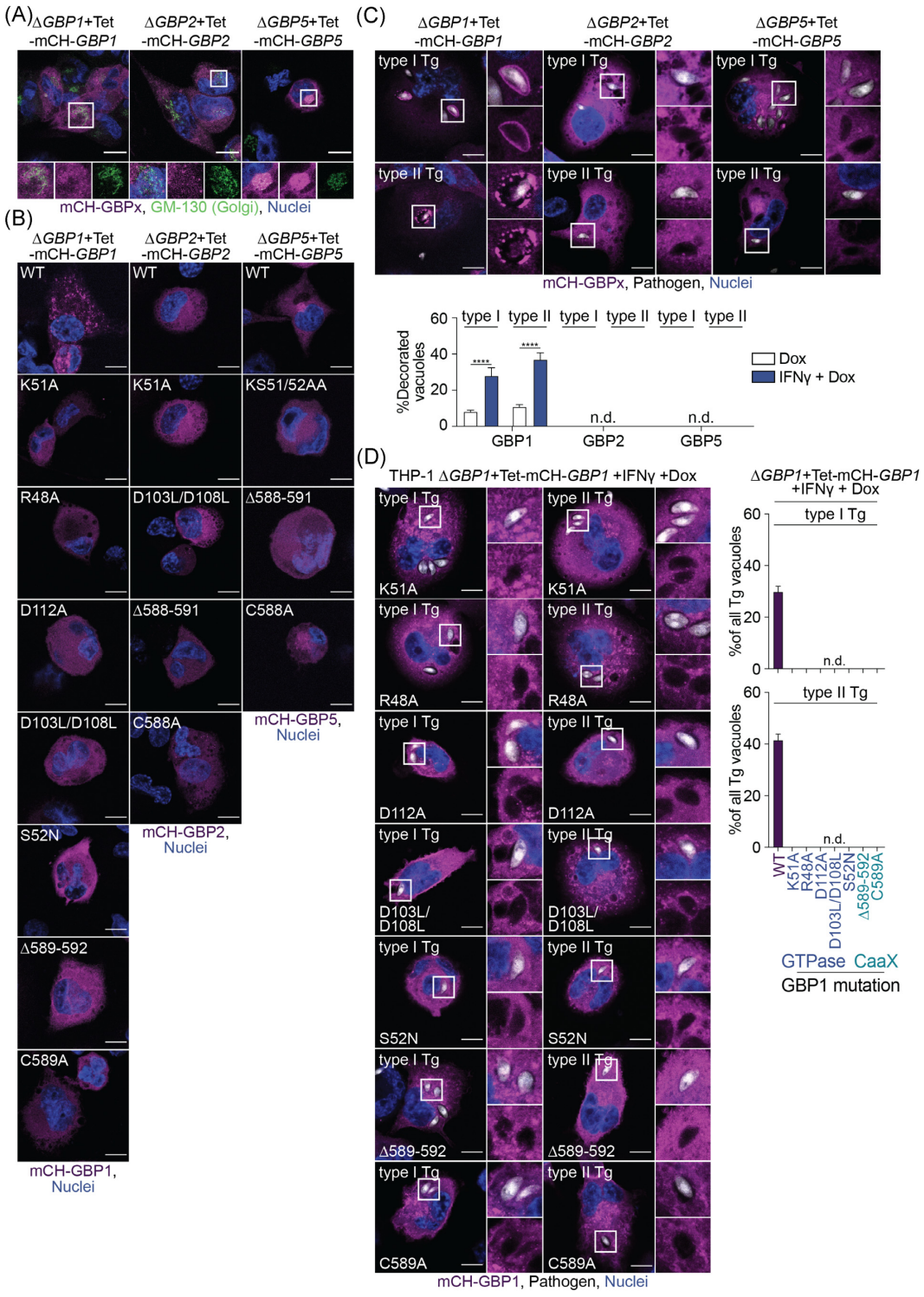

Figure 4. GBP2 and 5 do not localize to *Toxoplasma* vacuoles. **(A)** Immunofluorescence images of THP-1Δ*GBP1*+Tet-mCH-*GBP1*, Δ*GBP2*+Tet-mCH-*GBP2* or Δ*GBP5*+Tet-mCH-*GBP5* cells treated with IFNγ and Doxycycline (Dox) and stained for Golgi marker GM-130 to illustrate Golgi localization of GBP5 in uninfected cells. Magenta: mCherry (mCH)-GBP1/2/5; green: GM-130 (Golgi) and blue: nuclei. Scale bar, 10 μm. **(B)** Immunofluorescence images of THP-1Δ*GBP1*+Tet-mCH-*GBP1*, Δ*GBP2*+Tet-mCH-*GBP2* or Δ*GBP5*+Tet-mCH-*GBP5* cells expressing the indicated GBPx mutant treated with IFNγ+Dox to illustrate localization of the respective protein in uninfected cells. Magenta: mCherry (mCH)-GBP1/2/5 and blue: nuclei. Scale bar, 10 μm. **(C)** Immunofluorescence images (top) and HRMAn-based quantification of GBP recruitment to Tg (bottom) in THP-1Δ*GBP1*+Tet-mCH-*GBP1*, Δ*GBP2*+Tet-mCH-*GBP2* or Δ*GBP5*+Tet-mCH-*GBP5* cells treated with IFNγ+Dox and infected with type I (RH) or type II (PRU) *T. gondii* (Tg) for 6 h. Magenta: mCherry (mCH)-GBP1/2/5; grey: Tg and blue: nuclei. Scale bar, 10 μm. **(D)** Images (left) and HRMAn-based quantification of GBP1 recruitment to Tg-vacuoles (right) in THP-1Δ*GBP1*+Tet-mCH-*GBP1* cells expressing the indicated GBP1 mutant treated with IFNγ+Dox and infected for 6 h. Magenta: mCherry (mCH)-GBP1; grey: pathogen and blue: nuclei. Scale bar, 10 μm. Data information: images in (A + C-D) representative of $n = 3$ and in (B) representative of $n = 2$ independent experiments. Graph in (C + D) show mean ± SEM from $n = 3$ independent experiments. $^{****}P \leq 0.0001$ for indicated comparisons in (C) from one-way ANOVA comparing to Dox-only treated cells following adjustment for multiple comparisons; n.d. not detected.

apparatus, resembling prior observations in HeLa cells (Britzen-Laurent *et al.* 2010). It is known that correct localization of the three isoprenylated GBPs depends on lipidation with farnesyl (GBP1) or geranylgeranyl (GBP2/5; Britzen-Laurent *et al.* 2010). Accordingly, mutation of the CaaX box of either of the three GBPs led to uniform cytoplasmic distribution. Since GBP1/2/5 all show differing subcellular localizations despite all being isoprenylated, other parts of the proteins must contribute to their correct trafficking. One example could be the polybasic motif of GBP1 (R584–586), which when mutated led to the pronounced phenotype of protein aggregation, as also observed by other groups (Kohler *et al.* 2020; Kutsch *et al.* 2020).

GBP1, 2 and 5 have all been localized at the Golgi in previous studies (Modiano, Lu and Cresswell 2005; Tripal *et al.* 2007; Britzen-Laurent *et al.* 2010; Krapp *et al.* 2016; Braun *et al.* 2019). Aluminium fluoride treated HeLa cells or HFFs showed accumulation of GBP1 at the Golgi, suggesting that this only occurs in a GTP-locked conformation (Modiano, Lu and Cresswell 2005). GBP5 has a well-established localization at the Golgi and can further recruit GBP2 (Britzen-Laurent *et al.* 2010; Braun *et al.* 2019). In line with our results, isoprenylation of GBP5 was required for this. Localization of GBP5 at the Golgi is needed for its antiviral activity against HIV (Krapp *et al.* 2016), which is achieved by concerted action of GBP2 and GBP5, together reducing the activity of Furin protease (Braun *et al.* 2019). Since GBP5 GTPase and isoprenylation mutants lost their association with the Golgi apparatus, it is likely that GBP5 activity against Tg relies on its correct localization to the Golgi. Thus, GBP1/2/5 influence Tg growth by acting without accumulation of the proteins at the pathogen ('pathogen-distal'), which has been observed before for GBP1 in A549 lung-epithelial cells (Johnston *et al.* 2016) but contests the dogma of defense protein accumulation at the intracellular infection site (MacMicking 2012). It is tempting to speculate that the GBPs therefore have additional functions other than recruiting to pathogens.

Apart from Tg-restriction mechanism(s), GBP1 accumulated at Tg vacuoles in infected cells. Neither GBP2 nor GBP5 recruited to Tg. The recruitment of GBP1 was dependent on its GTPase function and isoprenylation. GBP1 recruitment might also rely on other proteins, as its association with Tg appears cell-type- and IFNγ-dependent. It will, therefore, be interesting to study GBP1-interactomes. Comparative study of macrophage and A549 lung epithelial cell GBP1-interactomes might offer the opportunity to identify critical GBP1 trafficking factors. Overall, recruitment of GBP1 to Tg resembles the function of its murine homologue, which is known to associate with bacterial pathogens (Kim *et al.* 2011; Haldar *et al.* 2014; Meunier *et al.* 2014, 2015; Finethy *et al.* 2015; Man *et al.* 2015; Feeley *et al.* 2017; Lindenberg *et al.* 2017; Wallet *et al.* 2017; Zwack *et al.* 2017; Balakrishnan *et al.* 2018; Liu *et al.* 2018) and Tg-PVs and was also found directly on the parasites (Virreira Winter *et al.* 2011; Kravets *et al.* 2012, 2016; Degrandi *et al.* 2013; Haldar *et al.* 2014, 2015; Costa Franco *et al.* 2018).

Careful examination of the effect of different mutations of the GBP1 GTPase activity (Praefcke *et al.* 2004; Modiano, Lu and Cresswell 2005; Abdullah, Balakumari and Sau 2010) revealed that full GTPase activity was needed for recruitment to Tg and killing of the pathogen, while GMP formation was dispensable for growth restriction. Interestingly, GBP1 was the only parasiticidal GBP family member, a function which may, therefore, rely on the formation of GMP. Similar observations have been made for *Chlamydia* infections, where GMP formation was necessary for GBP1-mediated pathogen and host-cell killing, but dispensable for *Chlamydia* growth restriction (Xavier *et al.* 2020). Conversely, GBP5 which cannot produce GMP (Wehner and Herrmann 2010), did not kill Tg. GBP2, however, which like GBP1, can hydrolyze GDP to GMP (Abdullah, Balakumari and Sau 2010), did not kill Tg. GTPase activity of GBP2 and GBP5 were nevertheless needed for Tg-growth restriction.

Taken together our results show that killing of Tg relies on GBP1 recruitment to the pathogens and a pathogen-proximal function involving the formation of GMP, whereas GBP1, 2 and 5 altogether restrict Tg-growth via a thus far unknown pathogen-distal function.

MATERIALS AND METHODS

Cell and parasite culture, treatments and infection

THP-1 (TIB202, ATCC) were maintained in RPMI with GlutaMAX (35050061, Gibco, Waltham, Massachusetts, USA) and 10% FBS (Sigma, Gillingham, UK), HFFs (SCRC 1041, ATCC) and HEK293T (Cell Services, The Francis Crick Institute, London, UK) were maintained in DMEM with GlutaMAX and 10% FBS at 37°C in 5% CO_2. THP-1s were differentiated with 50 ng/mL PMA (P1585, Sigma) for 3 days and then rested for 2 days in PMA-free, complete medium. All cells were regularly tested for mycoplasma by immunofluorescence and PCR. For a list of all cell lines see Table 1. Cells were stimulated for 16 h prior to infection with addition of 50 IU/mL human IFNγ (285-IF, R&D Systems, Abingdon, UK). Induction of GBP expression in the Dox-inducible cells was performed with 200 ng/mL Dox overnight (D9891, Sigma).

Tg were maintained by serial passage on HFF cell monolayers. Parasites were passaged onto new HFFs the day before infection. Tg were prepared from freshly 25G syringe lysed cultures by centrifugation at 50 × *g* for 3 min, transferring the cleared supernatant into a new tube, subsequent centrifugation at 500 × *g* for 7 min and re-suspension of the pelleted parasites into fresh complete medium. Parasite-suspension was added to the cells at a MOI of 1. Please note that the actual MOI in the experiment was probably higher (Fig. 2). The cell cultures with added Tg were then centrifuged at 500 × *g* for 5 min to synchronize infection. At 2 h post-infection, extracellular parasites were removed with three PBS washes (806552, Sigma) and fresh complete medium was added prior to culturing at 37°C, 5% CO_2 for the required time.

iPS cell culture and monocyte/macrophage production

The Kolf_2-C1 cell line (HPSI0114i-kolf_2-C1, https://hpscreg.eu/cell-line/WTSIi018-B-1) was obtained from the Wellcome Trust Sanger Institute. Production of monocytes from KOLF iPSC was previously described (Wilgenburg *et al.* 2013). KOLF cells were maintained in their pluripotent state in a feeder-free, serum-free culture system at 37°C in 5% CO_2 using Synthemax II-SC Substrate-coated plates (3535, Corning, Flintshire, UK) and mTeSR™-1 medium (85850, StemCell Technologies, Cambridge, UK). Cells were clump-passaged when colonies covered ∼75% of the wells by washing with PBS, detaching using Collagenase IV (07427, StemCell Technologies), followed by gentle scraping in mTeSR™-1 medium. Cells were split roughly 1:4 and supplemented with 1 mM Rock-inhibitor (Y27632; Calbiochem, Merck KGaA, Darmstadt, Germany). Cells were fed with new media daily.

To create monocyte production factories KOLF cells were washed with PBS and harvested with TrypLE Express (12604021, Gibco), dissociated into single cells by pipetting and finally diluted 1:10 with PBS and collected in a centrifuge tube. Cells

Table 1. List of cell lines.

Cells	Source
HEK 293T	Cell Services, Crick Institute
HFF	ATCC
KOLF iPSC	HESCU STP
THP-1	ATCC
THP-1 ΔGBP1	Fisch *et al.* (2019a)
THP-1 ΔGBP1 + Tet	Fisch *et al.* (2019a)
THP-1 ΔGBP1 + Tet-EV	Fisch *et al.* (2019a)
THP-1 ΔGBP1 + Tet-*GBP1*	Fisch *et al.* (2019a)
THP-1 ΔGBP1 + Tet-*GBP1*^{C589A}	Fisch *et al.* (2019a)
THP-1 ΔGBP1 + Tet-*GBP1*$^{D103L/D108L}$	This study
THP-1 ΔGBP1 + Tet-*GBP1*^{D112A}	This study
THP-1 ΔGBP1 + Tet-*GBP1*^{D184N}	This study
THP-1 ΔGBP1 + Tet-*GBP1*^{D192E}	Fisch *et al.* (2020)
THP-1 ΔGBP1 + Tet-*GBP1*^{E99A}	This study
THP-1 ΔGBP1 + Tet-*GBP1*^{K51A}	Fisch *et al.* (2019a)
THP-1 ΔGBP1 + Tet-*GBP1*^{R48A}	This study
THP-1 ΔGBP1 + Tet-*GBP1*^{R48P}	This study
THP-1 ΔGBP1 + Tet-*GBP1*$^{R584-586A}$	This study
THP-1 ΔGBP1 + Tet-*GBP1*$^{RK227/228EE}$	Fisch *et al.* (2019a)
THP-1 ΔGBP1 + Tet-*GBP1*^{S52N}	This study
THP-1 ΔGBP1 + Tet-*GBP1*^{T75A}	This study
THP-1 ΔGBP1 + Tet-*GBP1*$^{Δ589–592}$	Fisch *et al.* (2019a)
THP-1 ΔGBP1 + Tet-mCH-GBP1	Fisch *et al.* (2019a)
THP-1 ΔGBP1 + Tet-mCH-GBP1^{C589A}	Fisch *et al.* (2019a)
THP-1 ΔGBP1 + Tet-mCH-GBP1$^{D103L/D108L}$	This study
THP-1 ΔGBP1 + Tet-mCH-GBP1^{D112A}	This study
THP-1 ΔGBP1 + Tet-mCH-GBP1^{D192E}	Fisch *et al.* (2020)
THP-1 ΔGBP1 + Tet-mCH-GBP1^{K51A}	Fisch *et al.* (2019a)
THP-1 ΔGBP1 + Tet-mCH-GBP1^{R48A}	This study
THP-1 ΔGBP1 + Tet-mCH-GBP1$^{R584-586A}$	This study
THP-1 ΔGBP1 + Tet-mCH-GBP1$^{RK227/228EE}$	Fisch *et al.* (2019a)
THP-1 ΔGBP1 + Tet-mCH-GBP1^{S52N}	This study
THP-1 ΔGBP1 + Tet-mCH-GBP1$^{Δ589–592}$	Fisch *et al.* (2019a)
THP-1 ΔGBP2	This study
THP-1 ΔGBP2 + Tet	This study
THP-1 ΔGBP2 + Tet-EV	This study
THP-1 ΔGBP2 + Tet-*GBP2*	This study
THP-1 ΔGBP2 + Tet-*GBP2*$^{Δ588–591}$	This study
THP-1 ΔGBP2 + Tet-*GBP2*^{C588A}	This study
THP-1 ΔGBP2 + Tet-*GBP2*$^{D103L/D108L}$	This study
THP-1 ΔGBP2 + Tet-*GBP2*^{K51A}	This study
THP-1 ΔGBP2 + Tet-mCH-GBP2	This study
THP-1 ΔGBP2 + Tet-mCH-GBP2$^{Δ588–591}$	This study
THP-1 ΔGBP2 + Tet-mCH-GBP2^{C588A}	This study
THP-1 ΔGBP2 + Tet-mCH-GBP2$^{D103L/D108L}$	This study
THP-1 ΔGBP2 + Tet-mCH-GBP2^{K51A}	This study
THP-1 ΔGBP5	Krapp *et al.* (2016)
THP-1 ΔGBP5 + Tet	This study
THP-1 ΔGBP5 + Tet-EV	This study
THP-1 ΔGBP5 + Tet-*GBP5*	This study
THP-1 ΔGBP5 + Tet-*GBP5*$^{Δ588–591}$	This study
THP-1 ΔGBP5 + Tet-*GBP5*^{C588A}	This study
THP-1 ΔGBP5 + Tet-*GBP5*$^{KS51/52AA}$	This study
THP-1 ΔGBP5 + Tet-mCH-GBP5	This study
THP-1 ΔGBP5 + Tet-mCH-GBP5$^{Δ588–591}$	This study
THP-1 ΔGBP5 + Tet-mCH-GBP5^{C588A}	This study
THP-1 ΔGBP5 + Tet-mCH-GBP5$^{KS51/52AA}$	This study

were pelleted by centrifugation and resuspended in mTeSR™-1 supplemented with 1 mM Rock-inhibitor, 50 ng/mL BMP-4 (120–05, Peprotech, London, UK), 20 ng/mL SCF (130-093–991, Miltenyi, Bisley, UK) and 50 ng/mL VEGF (100–20, Peprotech; = EB medium). Next, AggreWell 800 plates (34811, StemCell Technologies) were prepared by rinsing with PBS, addition of 1 mL EB medium to each well and centrifugation at 3,000× *g* for 2 min. Then, 1 mL of harvested cells were added per well, the plate centrifuged at 150 × *g* for 3 min and left in the incubator for 4 days. EBs were fed daily with fresh EB medium by stepwise exchanging 75% of medium. EBs were harvested by dislodging through pipetting, transferring the well-contents onto a 40 mm strainer, rinsing with PBS and collecting them into a new tube. A total of 500 EBs were transferred per T175 tissue culture flasks in 20 mL X-VIVO15 (04–418Q, Lonza), supplemented with 100 ng/mL M-CSF (PHC9504, Gibco), 25 ng/mL IL-3 (203-GMP, R&D Systems), 2 mM GlutaMAX, 100 U/mL penicillin/streptomycin (15140122, Invitrogen, Renfrew, UK) and 0.05 mM β-Mercaptoethanol (21985023, Gibco). Roughly 2–3 weeks following seeding monocytes in suspension appeared and were harvested fortnightly from the supernatant. Monocytes were differentiated into macrophages in X-VIVO15 supplemented with 100 ng/mL M-CSF for 5 days.

Primary human macrophage isolation and culture

PBMCs were extracted from Leukocyte cones from healthy donors (NHS) via Ficoll (17544202, GE Healthcare, Chalfont Saint Giles, UK) density gradient centrifugation. $CD14^+$ monocytes were extracted using magnetic microbeads (130–050-201, MACS Miltenyi, Bisley, UK). Monocytes were counted, seeded and differentiated for 1 week in RPMI containing 10% human AB serum (H4522, Sigma), GlutaMAX, penicillin/streptomycin and 5 ng/mL hGM-CSF (130–093-864, Miltenyi). The medium was replaced after 2 and 5 days, to replenish the hGM-CSF.

siRNA transfection

Cells were transfected 2 days prior to infection, at the time the THP-1 differentiation medium was replaced, or MDM/iPSC differentiation medium was replaced on day 5 after seeding. All siRNAs were used at a final concentration of 30 nM. To set up the transfection mix, a 10X mix was prepared in OptiMEM containing the appropriate siRNA(s) and TransIT-X2 transfection reagent (MIR600, Mirus) in a 1:2 stoichiometry. As the GBPs exhibit high sequence similarity, a costum transfection panel using three different Silencer Select siRNAs (Ambion: GBP1: s5620, s5621 and s5622; GBP2: s5623, s5624 and s5625; GBP3: s5626, s5627 and s5628; GBP4: s41805, s41806 and s41807; GBP5: s41808, s41809 and s41810) was used (Fisch *et al.* 2019a). The appropriate negative control was Silencer Select Negative Control No. 1 siRNA (#4390843, Ambion, Thermo Fisher Scientific, Horsham, UK).

Plaque assays

A total of 0.8×10^6 differentiated THP-1 cells were infected with Tg as described above and 18 h p.i. supernatant and cells were harvested from the wells of a 12-well plate. Cells were syringe-lysed and obtained parasites from within the cells and the supernatant diluted 1:10,000 and added to HFFs grown confluent in wells of a 24-well plate.

Determination of plaque sizes and number was performed 5 days p.i. of the HFFs, when cells were fixed with ice-cold methanol and stained with crystal violet (C6158, Sigma). Following five washes with PBS, plaques were imaged on a GelCount Colony Counter (Oxford Optronix, Abingdon, UK) and cell covered area determined using FIJI. Proportions of plaque and plaque loss, as compared to Tg grown in untreated THP-1, were calculated.

Table 2. List of qPCR primers.

Name	Sequence 5′-3′
GBP1-fwd	TATTGCCCACTATGAACAGCAGAT
GBP1-rev	TAGCTGGGCCGCTAACTCC
GBP2-fwd	AATTAGGGGCCCAGTTGGAAG
GBP2-rev	AAGAGACGGTAACCTCCTGGT
GBP3-fwd	GAATAAGGGCTTCTCTCTGGGC
GBP3-rev	AGTGTCAAGCAGGACTAAGGTG
GBP4-fwd	TAAGCGGCTTTCAGAGCACC
GBP4-rev	GACCTCGTTTGCCTTAACTCC
GBP5-fwd	CCTGATGATGAGCTAGAGCCTG
GBP5-rev	GCACCAGGTTCTTTAGACGAGA
GBP6-fwd	TGCACCATCCCATTTGTGGAA
GBP6-rev	TGCCAACCTAGAAGAGCCTGC
GBP7-fwd	GAGTTAAGGCAGACGAGGTCC
GBP7-rev	TTCAGCTGCCTCCTTCTTAGC
HPRT1-fwd	ACCAGTCAACAGGGGACATAA
HPRT1-rev	CTTCGTGGGGTCCTTTTCACC

Flow cytometry

A total of 1×10^6 differentiated macrophages were harvested using accutase (A6964, Sigma) and scraping and washed twice with warm PBS. Cells were resuspended in PBS + 1% BSA containing dilutions of fluorescently labelled antibodies against surface receptors and incubated for 1 h at room temperature in the dark. Cells were washed with PBS, fixed with 4% formaldehyde for 15 min at room temperature and washed again, prior to resuspension in PBS + 1% BSA. All samples were analysed on a LSR Fortessa (BD Biosciences, Wokingham, UK), and recorded data was processed using FlowJo 10.3 (FlowJo, LLC, Ashland, US).

RT-qPCR

RNA was extracted from 0.25×10^6 cells using Trizol reagent (15596026, Invitrogen). A total of 5 μg/mL GlycoBlue (AM9516, Invitrogen) was added during the isopropanol (190764, Sigma) precipitation to increase RNA-yields. RNA quality was measured on a Nanodrop 2000 Spectrophotometer (Thermo Fisher Scientific, Horsham, UK). A total of 1 μg RNA was reverse transcribed using high-capacity cDNA synthesis kit (4368813, Applied Biosystems, Waltham, US). qPCR used PowerUP SYBR green (A25742, Applied Biosystems), 20 ng cDNA in a 20 μL reaction and primers at 1 μM final concentration on a QuantStudio 12K Flex Real-Time PCR System (Applied Biosystems). Primer specificity was ensured by designing primers to span exon–exon junctions, whenever possible, and for each primer pair a melt curve was recorded (see Table 2). Ct values were normalized to the Ct of human *HPRT1*, and data plotted as ΔCt (Relative expression). To determine absolute expression of GBPs, a defined amount of linearized plasmid standards was added as PCR template and obtained Ct values used to calculate transcript numbers from the samples.

Table 3. List of primary antibodies.

Antibody	IF	IB	FC	Supplier	Catalog number
Actin		x		Sigma	A2228
CD14			x	Biolegend	#325607
CD16			x	Biolegend	#302005
CD68			x	Biolegend	#137027
GBP1 (mAb)	x	x		Home-made	
GBP1 (pAb)		x		Home-made	
GBP2		x		Santa cruz	sc-271568
GBP5		x		CST	#67798
GM-130	x			Abcam	ab52649
mCherry		x		Abcam	ab167453

IF: immunofluorescence; IB = immunoblotting and FC: flow cytometry.

Creation of new cell lines

THP-1Δ*GBP1* and the Dox-inducible system were previously published (Fisch *et al*. 2019a). THP-1Δ*GBP5* were a gift from Frank Kirchhoff (Krapp *et al*. 2016). Guide RNA (gRNA) sequences targeting the 5′ and 3′ UTR of *GBP2* gene were designed using cripr.mit.edu. DNA oligonucleotides encoding for the crRNAs (sgRNA1: 5′- CACCGTGTCTTACAAATTGGGTCAC-3′; sgRNA2: 5′- CACCGCATGAGTTGAATTGCTCTGT-3′) were annealed by mixing in equimolar ratio and boiling at 95°C for 15 min followed by a slow decrease to room temperature. Annealed oligos were then cloned into BsmBI-digested (ER0451, Thermo Scientific) pLentiCRISPR-V2 backbone (Sanjana, Shalem and Zhang 2014) using Quick Ligation kit (M2200, NEB, Ipswich, US) and transduced into THP-1 WT cells using Lentiviral particles (Fisch *et al*. 2019a). Following selection with 1 μg/mL Puromycin (A1113802, Gibco) for 14 days, cells were sub-cloned by serial dilution into ten 96-well plates using pre-conditioned complete medium supplemented with non-essential amino acids (11140076, Gibco), penicillin/streptomycin and GlutaMAX. Roughly 3 weeks after seeding of the single cells, obtained clones were expanded into 24-well plates with 2 mL fresh medium and screened for absence of *GBP2* expression by RT-qPCR. Clones that showed reduced or absent *GBP2* expression underwent secondary screening by immunoblotting. Finally, confirmed KO clones were tested again by Sanger sequencing of the genomic target locus, RT-qPCR and immunoblotting.

Cells with Dox-inducible GBP expression were created as previously published (Fisch *et al*. 2019a). To create plasmids that express GBP1, GBP2 or GBP5 under the control of Dox, RNA from IFNγ-treated THP-1s was extracted and cDNA synthesized as described above. The CDS of *GBP* mRNA was amplified with Q5 polymerase, the amplicon treated with Taq polymerase (M0273, NEB) to create A-overhangs and cloned into pCR2.1®-TOPO TA vector using TOPO TA kit (451641, Invitrogen). GBP mutants were created by site-directed mutagenesis, introducing single point mutations with mismatch-primers and PCR with Q5 polymerase. Using the mutated or wildtype GBP-containing vectors, the ORFs were PCR-amplified to create overhangs to pLenti-Tet vector. Gibson assemblies of the digested backbone and the *GBP* ORFs were performed, and successful cloning confirmed by Sanger sequencing. To create mCH-tagged versions, mCH-ORF was amplified with overlaps to the backbone and the *GBP* ORF and included in the Gibson assembly reactions. *GBP* ORFs lacking the C-terminal CaaX-box were amplified with primers excluding parts of the wildtype *GBP* ORFs.

SDS-PAGE and immunoblotting

A total of 0.5 × 10^6 cells were seeded per well of a 48-well plate, differentiated and treated as described above. At the end of treatments, cells were washed with ice-cold PBS and lysed for 5 min on ice in 50 μL RIPA buffer (150 mM NaCl, 1% Nonidet P-40, 0.5% sodium deoxycholate, 0.1% SDS and 25 mM Tris-HCl pH 7.4) supplemented with protease inhibitors (Protease Inhibitor Cocktail set III, EDTA free, Merck, Darmstadt, Germany) and PhosSTOP phosphatase inhibitors (4906845001, Roche, Basel, Switzerland). Lysates were cleared by centrifugation at full speed for 15 min at 4°C. BCA assay (Pierce BCA protein assay kit, 23225, Thermo Scientific) was performed to determine protein concentrations. A total of 10 μg of total protein per sample were mixed with Laemmli buffer (#1610737, Bio-Rad) containing 5% DTT (646563–10X, Sigma) and boiled at 95°C for 10 min and then run on Bis-Tris gels (Novex, Invitrogen) in MOPS running buffer.

Following SDS-PAGE, proteins were transferred onto Nitrocellulose membranes using iBlot transfer system (Invitrogen). Membranes were blocked with either 5% BSA (A2058, Sigma) or 5% dry-milk (M7409, Sigma) in TBS-T (0.05% Tween-20) for at least 1 h at room temperature. Incubation with primary Abs (see Table 3) was performed at 4°C overnight. Blots were developed by washing the membranes with TBS-T, probed with 1:5,000 diluted HRP-conjugated secondary Abs in 5% BSA in TBS-T and washed again. Finally, the membranes were incubated for 2 min with ECL (Immobilon Western, WBKLS0500, Millipore, Burlington, USA) and chemiluminescence recorded on a ChemiDoc MP imaging system (Bio-Rad, Hercules, US).

Microscopy

In total, 0.25 × 10^6 cells were seeded on gelatin-coated (G1890, Sigma) coverslips in 24-well plates. Following differentiation, treatments and infection, cells were washed three times with warm PBS, prior to fixation, to remove any uninvaded pathogens and then fixed with 4% methanol-free formaldehyde (28906, Thermo Scientific) for 15 min at room temperature. For high-throughput imaging 50,000 cells were seeded of a black-wall, clear bottom 96-well imaging plate (Thermo Scientific), differentiated and treated and fixed as described above.

Following fixation, cells were washed again with PBS and kept at 4°C overnight to quench any unreacted formaldehyde. Fixed specimens were permeabilized with PermQuench buffer (0.2% (w/v) BSA and 0.02% (w/v) saponin in PBS) for 30 min

at room temperature and then stained with primary Abs (see Table 3) for 1 h at room temperature. After three washes with PBS, cells were incubated with the appropriated fluorescently labeled secondary Ab and 1 μg/mL Hoechst 33342 (H3570, Invitrogen) diluted in PermQuench buffer for 1 h at room temperature. Cells were washed with PBS five times and mounted using 5 μL Mowiol. For high-throughput imaging, fixed and permeabilized specimens were stained for 1 h at room temperature by adding PermQuench buffer containing 1 μg/mL Hoechst 33342 and 2 μg/mL CellMask Deep Red plasma membrane stain (H32721, Invitrogen). After staining, the specimens were washed with PBS five times and kept in 200 μL PBS per well for imaging.

Coverslips were imaged on a Leica SP5-inverted confocal microscope using 100× magnification and analysed using LAS-AF software. Plates were imaged on a Cell Insight CX7 High-Content Screening (HCS) Platform (Thermo Scientific) using 20× magnification. Following acquisition, images were exported from HCS Studio Cell Analysis as single channel 16-bit .tiff files before they were fed into the HRMAn (Fisch *et al.* 2019b, 2021) analysis pipeline.

Data handling and statistics

Data was plotted using Prism 8.4.0 (GraphPad Inc., San Diego, US) and presented as means of $n = 3$ experiments (with usually three technical repeats within each experiment) with error bars as standard error of the mean (SEM), unless stated otherwise. Significance of results was determined by non-parametric one-way ANOVA or two-way ANOVA as indicated in the figure legends. Benjamini, Krieger and Yekutieli false-discovery rate (Q = 5%) based correction for multiple comparisons as implemented in Prism was used when making more than three comparisons.

SUPPLEMENTARY DATA

Supplementary data are available at *FEMSPD* online.

AUTHOR CONTRIBUTION

DF and EMF conceived the project. DF conducted the experiments. BC set up and assisted with imaging experiments. RK and LH set up initial iPS cell culture. DF and EMF wrote the manuscript. EMF supervised the project. EMF acquired funding related to the project.

ACKNOWLEDGMENTS

We would like to thank Dr Mike Howell at the Francis Crick Institute for help with high-throughput image acquisition, Dr Sally Cowley for providing the iPSC macrophage protocol and Dr Nashied Peton and Dr Anna Coussens for advice on MDM production. We would also like to thank past and present members of the Frickel lab for critical discussion of this study.

FUNDING

This research was funded, in whole or in part, by The Wellcome Trust. A CC BY license is applied to the AAM arising from this submission, in accordance with the grant's open access conditions. EMF is supported by a Wellcome Trust Senior Research Fellowship (217202/Z/19/Z). This work was supported by the Francis Crick Institute, which receives its core funding from Cancer Research UK (FC001076 to EMF and FC001999 to LH), the UK Medical Research Council (FC001076 to EMF and FC001999 to LH) and the Wellcome Trust (FC001076 to EMF and FC001999 to LH). DF was supported by a Boehringer Ingelheim Fonds PhD fellowship. EMF acknowledges The Wellcome Trust Sanger Institute as the source of HPSI0114i-kolf_2-C1 human-induced pluripotent cell line which was generated under the Human Induced Pluripotent Stem Cell Initiative funded by a grant from the Wellcome Trust and Medical Research Council, supported by the Wellcome Trust (WT098051) and the NIHR/Wellcome Trust Clinical Research Facility, and acknowledges Life Science Technologies Corporation as the provider of Cytotune.

Conflicts of Interest. None declared.

REFERENCES

Abdullah N, Balakumari M, Sau AK. Dimerization and its role in GMP formation by human guanylate binding proteins. *Biophys J* 2010;**99**:2235–44.

Balakrishnan A, Karki R, Berwin B *et al.* Guanylate binding proteins facilitate caspase-11-dependent pyroptosis in response to type 3 secretion system-negative *Pseudomonas aeruginosa*. *Cell Death Discov* 2018;**4**:66.

Barz B, Loschwitz J, Strodel B. Large-scale, dynamin-like motions of the human guanylate binding protein 1 revealed by multi-resolution simulations. Kasson PM (ed). *PLoS Comput Biol* 2019;**15**:e1007193.

Ben-David U, Siranosian B, Ha G *et al.* Genetic and transcriptional evolution alters cancer cell line drug response. *Nat 2018 5607718* 2018;**560**:325–30.

Boehm U, Guethlein L, Klamp T *et al.* Two families of GTPases dominate the complex cellular response to IFN-gamma. *J Immunol* 1998;**161**:6715–23.

Braun E, Hotter D, Koepke L *et al.* Guanylate-binding proteins 2 and 5 exert broad antiviral activity by inhibiting furin-mediated processing of viral envelope proteins. *Cell Rep* 2019;**27**:2092–104.

Britzen-Laurent N, Bauer M, Berton V *et al.* Intracellular trafficking of guanylate-binding proteins is regulated by heterodimerization in a hierarchical manner. *PLoS ONE* 2010;**5**:e14246.

Chanput W, Mes JJ, Wichers HJ. THP-1 cell line: an in vitro cell model for immune modulation approach. *Int Immunopharmacol* 2014;**23**:37–45.

Cheng YSE, Becker-Manley MF, Chow TP *et al.* Affinity purification of an interferon-induced human guanylate-binding protein and its characterization. *J Biol Chem* 1985;**260**:15834–9.

Clough B, Frickel E-M. The toxoplasma parasitophorous vacuole: an evolving host-parasite frontier. *Trends Parasitol* 2017;**33**:473–88.

Costa Franco MM, Marim F, Guimarães ES *et al. Brucella abortus* triggers a cGAS-Independent STING pathway to induce host protection that involves guanylate-binding proteins and inflammasome activation. *J Immunol* 2018;**200**:607–22.

Cronkite DA, Strutt TM. The regulation of inflammation by innate and adaptive lymphocytes. *J Immunol Res* 2018;**2018**:e1467538.

Daffos F, Forestier F, Capella-Pavlovsky M *et al.* Prenatal management of 746 pregnancies at risk for congenital toxoplasmosis. *N Engl J Med* 1988;**318**:271–5.

Darnell JE, Kerr IM, Stark GR. Jak-STAT pathways and transcriptional activation in response to IFNs and other extracellular signaling proteins. *Science* 1994;**264**:1415–21.

Degrandi D, Kravets E, Konermann C *et al*. Murine guanylate binding protein 2 (mGBP2) controls *Toxoplasma gondii* replication. *Proc Natl Acad Sci USA* 2013;**110**:294–9.

Desmonts G, Forestier F, Thulliez P *et al*. Prenatal diagnosis of congenital toxoplasmosis. *Lancet* 1985;**325**:500–4.

Dinarello CA. Historical insights into cytokines. *Eur J Immunol* 2007;**37**:S34–45.

Feeley EM, Pilla-Moffett DM, Zwack EE *et al*. Galectin-3 directs antimicrobial guanylate binding proteins to vacuoles furnished with bacterial secretion systems. *Proc Natl Acad Sci USA* 2017;**114**:E1698–706.

Feghali CA, Wright TM. Cytokines in acute and chronic inflammation. *Front Biosci* 1997;**2**. DOI: 10.2741/a171.

Finethy R, Jorgensen I, Haldar AK *et al*. Guanylate binding proteins enable rapid activation of canonical and noncanonical inflammasomes in Chlamydia-infected macrophages. *Infect Immun* 2015;**83**:4740–9.

Fisch D, Bando H, Clough B *et al*. Human GBP1 is a microbe-specific gatekeeper of macrophage apoptosis and pyroptosis. *EMBO J* 2019a;**38**:e100926.

Fisch D, Clough B, Domart M-C *et al*. Human GBP1 differentially targets salmonella and toxoplasma to license recognition of microbial ligands and caspase-mediated death. *Cell Rep* 2020;**32**:1–14.

Fisch D, Evans R, Clough B *et al*. HRMAn 2.0: next-generation artificial intelligence–driven analysis for broad host–pathogen interactions. *Cell Microbiol* 2021;**23**:e13349.

Fisch D, Yakimovich A, Clough B *et al*. Defining host–pathogen interactions employing an artificial intelligence workflow. *Elife* 2019b;**8**:e40560.

Gazzinelli RT, Hieny S, Wynn TA *et al*. Interleukin 12 is required for the T-lymphocyte-independent induction of interferon γ by an intracellular parasite and induces resistance in T-cell- deficient hosts. *Proc Natl Acad Sci USA* 1993;**90**:6115–9.

Gazzinelli RT, Wysocka M, Hayashi S *et al*. Parasite-induced IL-12 stimulates early IFN-gamma synthesis and resistance during acute infection with *Toxoplasma gondii*. *J Immunol* 1994;**153**:2533–43.

Ghosh A, Praefcke GJKK, Renault L *et al*. How guanylate-binding proteins achieve assembly-stimulated processive cleavage of GTP to GMP. *Nature* 2006;**440**:101–4.

Green DR, Oguin TH, Martinez J. The clearance of dying cells: table for two. *Cell Death Differ* 2016;**23**:915–26.

Haldar AK, Foltz C, Finethy R *et al*. Ubiquitin systems mark pathogen-containing vacuoles as targets for host defense by guanylate binding proteins. *Proc Natl Acad Sci USA* 2015;**112**:E5628–37.

Haldar AK, Piro AS, Finethy R *et al*. *Chlamydia trachomatis* is resistant to inclusion ubiquitination and associated host defense in gamma interferon-primed human epithelial cells. *MBio* 2016;**7**:e01417–16.

Haldar AK, Piro AS, Pilla DM *et al*. The E2-like conjugation enzyme atg3 promotes binding of IRG and gbp proteins to Chlamydia- and Toxoplasma-containing vacuoles and host resistance. *PLoS ONE* 2014;**9**:e86684.

Haldar AK, Saka HA, Piro AS *et al*. IRG and GBP host resistance factors target aberrant, non-self vacuoles characterized by the missing of self IRGM proteins. *PLoS Pathog* 2013;**9**:e1003414.

Howe DK, Sibley LD. *Toxoplasma gondii* comprises three clonal lineages: correlation of parasite genotype with human disease. *J Infect Dis* 1995;**172**:1561–6.

Hughes CE, Benson RA, Bedaj M *et al*. Antigen-presenting cells and antigen presentation in tertiary lymphoid organs. *Front Immunol* 2016;**7**. DOI: 10.3389/fimmu.2016.00481.

Hunn JP, Koenen-Waisman S, Papic N *et al*. Regulatory interactions between IRG resistance GTPases in the cellular response to *Toxoplasma gondii*. *EMBO J* 2008;**27**:2495–509.

Hunter CA, Subauste CS, Van Cleave VH *et al*. Production of gamma interferon by natural killer cells from *Toxoplasma gondii*-infected SCID mice: regulation by interleukin-10, interleukin-12, and tumor necrosis factor alpha. *Infect Immun* 1994;**62**:2818–24.

Ince S, Kutsch M, Shydlovskyi S *et al*. The human guanylate-binding proteins hGBP-1 and hGBP-5 cycle between monomers and dimers only. *FEBS J* 2017;**284**:2284–301.

Ince S, Zhang P, Kutsch M *et al*. Catalytic activity of human guanylate-binding protein 1 coupled to the release of structural restraints imposed by the C-terminal domain. *FEBS J* 2020. DOI: 10.1111/febs.15348.

Ivashkiv LB. IFNγ: signalling, epigenetics and roles in immunity, metabolism, disease and cancer immunotherapy. *Nat Rev Immunol* 2018;**18**:545–58.

Johnston AC, Piro A, Clough B *et al*. Human GBP1 does not localize to pathogen vacuoles but restricts *Toxoplasma gondii*. *Cell Microbiol* 2016;**18**:1056–64.

Kim B-H, Shenoy AR, Kumar P *et al*. A family of IFN-γ–Inducible 65-kD GTPases protects against bacterial infection. *Science* 2011;**332**:717–21.

Kohler KM, Kutsch M, Piro AS *et al*. A rapidly evolving polybasic motif modulates bacterial detection by guanylate binding proteins. *MBio* 2020;**11**:1–14.

Krapp C, Hotter D, Gawanbacht A *et al*. Guanylate binding protein (GBP) 5 is an interferon-inducible inhibitor of HIV-1 infectivity. *Cell Host Microbe* 2016;**19**:504–14.

Kravets E, Degrandi D, Ma Q *et al*. Guanylate binding proteins directly attack *Toxoplasma gondii* via supramolecular complexes. *Elife* 2016;**5**:e11479.

Kravets E, Degrandi D, Weidtkamp-Peters S *et al*. The GTPase activity of murine guanylate-binding protein 2 (mGBP2) controls the intracellular localization and recruitment to the parasitophorous vacuole of *Toxoplasma gondii*. *J Biol Chem* 2012;**287**:27452–66.

Kutsch M, Sistemich L, Lesser CF *et al*. Direct binding of polymeric GBP1 to LPS disrupts bacterial cell envelope functions. *EMBO J* 2020:e104926.

Lehmann T, Marcet PL, Graham DH *et al*. Globalization and the population structure of *Toxoplasma gondii*. *Proc Natl Acad Sci USA* 2006;**103**:11423–8.

Lindenberg V, Mölleken K, Kravets E *et al*. Broad recruitment of mGBP family members to *Chlamydia trachomatis* inclusions. *PLoS ONE* 2017;**12**:e0185273. Dean D (ed).

Liu BC, Sarhan J, Panda A *et al*. Constitutive interferon maintains GBP expression required for release of bacterial components upstream of pyroptosis and anti-DNA responses. *Cell Rep* 2018;**24**:155–68.

MacMicking JD. Interferon-inducible effector mechanisms in cell-autonomous immunity. *Nat Rev Immunol* 2012;**12**:367–82.

Man SM, Karki R, Malireddi RKS *et al*. The transcription factor IRF1 and guanylate-binding proteins target activation of the AIM2 inflammasome by francisella infection. *Nat Immunol* 2015;**16**:467–75.

Matta SK, Patten K, Wang Q *et al*. NADPH oxidase and guanylate binding protein 5 restrict survival of avirulent type III strains of *Toxoplasma gondii* in naive macrophages. *MBio* 2018;**9**:01393–18.

Meunier E, Dick MS, Dreier RF *et al.* Caspase-11 activation requires lysis of pathogen-containing vacuoles by IFN-induced GTPases. *Nature* 2014;**509**:366–70.

Meunier E, Wallet P, Dreier RF *et al.* Guanylate-binding proteins promote activation of the AIM2 inflammasome during infection with *Francisella novicida*. *Nat Immunol* 2015;**16**:476–84.

Modiano N, Lu YE, Cresswell P. Golgi targeting of human guanylate-binding protein-1 requires nucleotide binding, isoprenylation, and an IFN-γ-inducible cofactor. *Proc Natl Acad Sci USA* 2005;**102**:8680–5.

Nantais DE, Schwemmle M, Stickney JT *et al.* Prenylation of an interferon-γ-induced GTP-binding protein: the human guanylate binding protein, huGBP1. *J Leukoc Biol* 1996;**60**: 423–31.

Noronha N, Ehx G, Meunier M-C *et al.* Major multilevel molecular divergence between THP-1 cells from different biorepositories. *Int J Cancer* 2020;**147**:2000–6.

Olszewski MA, Gray J, Vestal DJ. In silico genomic analysis of the human and murine guanylate-binding protein (GBP) gene clusters. *J Interf Cytokine* 2006;**26**:328–52.

Pappas G, Roussos N, Falagas ME. Toxoplasmosis snapshots: global status of *Toxoplasma gondii* seroprevalence and implications for pregnancy and congenital toxoplasmosis. *Int J Parasitol* 2009;**39**:1385–94.

Park EK, Jung HS, Yang HI *et al.* Optimized THP-1 differentiation is required for the detection of responses to weak stimuli. *Inflamm Res* 2007;**56**:45–50.

Pena HFJ, Gennari SM, Dubey JP *et al.* Population structure and mouse-virulence of *Toxoplasma gondii* in Brazil. *Int J Parasitol* 2008;**38**:561–9.

Piro AS, Hernandez D, Luoma S *et al.* Detection of cytosolic *Shigella flexneri* via a C-terminal triple-arginine motif of GBP1 inhibits actin-based motility. *MBio* 2017;**8**. DOI: 10.1128/mBio.01979-17.

Praefcke GJK, Kloep S, Benscheid U *et al.* Identification of residues in the human guanylate-binding protein 1 critical for nucleotide binding and cooperative GTP hydrolysis. *J Mol Biol* 2004;**344**:257–69.

Prakash B, Praefcke GJK, Renault L *et al.* Structure of human guanylate-binding protein 1 representing a unique class of GTP-binding proteins. *Nature* 2000;**403**:567–71.

Qin A, Lai D-H, Liu Q *et al.* Guanylate-binding protein 1 (GBP1) contributes to the immunity of human mesenchymal stromal cells against *Toxoplasma gondii*. *Proc Natl Acad Sci USA* 2017;**114**:1365–70.

Remington JS, McLeod R, Wilson CB *et al.* Toxoplasmosis. In: Remington JS, Klein J (eds). *Infectious Diseases of the Fetus and Newborn Infant*, 2011, 918–1041.

Roche PA, Furuta K. The ins and outs of MHC class II-mediated antigen processing and presentation. *Nat Rev Immunol* 2015;**15**:203–16.

Rosales C, Uribe-Querol E. Phagocytosis: a fundamental process in immunity. *Biomed Res Int* 2017;**2017**. DOI: 10.1155/2017/9042851.

Ryves WJ, Evans AT, Olivier AR *et al.* Activation of the PKC-isotypes alpha, beta 1, gamma, delta and epsilon by phorbol esters of different biological activities. *FEBS Lett* 1991;**288**:5–9.

Sanjana NE, Shalem O, Zhang F. Improved vectors and genome-wide libraries for CRISPR screening. *Nat Methods* 2014;**11**: 783–4.

Schwemmle M, Staeheli P. The interferon-induced 67-kDa guanylate-binding protein (hGBP1) is a GTPase that converts GTP to GMP. *J Biol Chem* 1994;**269**:11299–305.

Sibley DL. Invasion and intracellular survival by protozoan parasites. *Immunol Rev* 2011;**240**:72–91.

Sibley LD, Ajioka JW. Population structure of *Toxoplasma gondii*: clonal expansion driven by infrequent recombination and selective sweeps. *Annu Rev Microbiol* 2008;**62**:329–51.

Sibley LD, Boothroyd JC. Virulent strains of *Toxoplasma gondii* comprise a single clonal lineage. *Nature* 1992;**359**:82–5.

Su C, Khan A, Zhou P *et al.* Globally diverse *Toxoplasma gondii* isolates comprise six major clades originating from a small number of distinct ancestral lineages. *Proc Natl Acad Sci USA* 2012;**109**:5844–9.

Tedesco S, De Majo F, Kim J *et al.* Convenience versus biological significance: are PMA-differentiated THP-1 cells a reliable substitute for blood-derived macrophages when studying in vitro polarization? *Front Pharmacol* 2018;**9**:71.

Tretina K, Park E, Maminska A *et al.* Interferon-induced guanylate-binding proteins : guardians of host defense in health and disease. *J Exp Med* 2019;**216**: 1–19.

Tripal P, Bauer M, Naschberger E *et al.* Unique features of different members of the human guanylate-binding protein family. *J Interf cytokine Res* 2007;**27**:44–52.

Turner MD, Nedjai B, Hurst T *et al.* Cytokines and chemokines: at the crossroads of cell signalling and inflammatory disease. *Biochim Biophys Acta Mol Cell Res* 2014;**1843**:2563–82.

Uhlen M, Fagerberg L, Hallstrom BM *et al.* Tissue-based map of the human proteome. *Science* 2015;**347**:1260419–.

Virreira Winter S, Niedelman W, Jensen KD *et al.* Determinants of GBP recruitment to Toxoplasma gondii vacuoles and the parasitic factors that control it. Moreno SN (ed). *PLoS ONE* 2011;**6**:e24434.

Wallet P, Benaoudia S, Mosnier A *et al.* IFN-γ extends the immune functions of guanylate binding proteins to inflammasome-independent antibacterial activities during *Francisella novicida* infection. *PLoS Pathog* 2017:1–26.

Wandel MP, Pathe C, Werner EI *et al.* GBPs inhibit motility of *Shigella flexneri* but are targeted for degradation by the bacterial ubiquitin ligase IpaH9. *Cell Host Microbe* 2017;**22**:507–18.

Wehner M, Herrmann C. Biochemical properties of the human guanylate binding protein 5 and a tumor-specific truncated splice variant. *FEBS J* 2010;**277**:1597–605.

Wilgenburg B van, Browne C, Vowles J *et al.* Efficient, long term production of monocyte-derived macrophages from human pluripotent stem cells under partly-defined and fully-defined conditions. Covas DT (ed). *PLoS ONE* 2013;**8**:e71098.

Wilson DC, Matthews S, Yap GS. IL-12 signaling drives CD8 + t cell IFN-γ production and differentiation of KLRG1 + effector subpopulations during *Toxoplasma gondii* infection. *J Immunol* 2008;**180**:5935–45.

Wynn TA, Chawla A, Pollard JW. Macrophage biology in development, homeostasis and disease. *Nature* 2013;**496**:445–55.

Xavier A, Al-Zeer MA, Meyer TF *et al.* hGBP1 coordinates chlamydia restriction and inflammasome activation through sequential GTP hydrolysis. *Cell Rep* 2020;**31**:107667.

Zwack EE, Feeley EM, Burton AR *et al.* Guanylate binding proteins regulate inflammasome activation in response to hyperinjected Yersinia translocon components. *Infect Immun* 2017;**85**:e00778–16.